CIWC 2019

sciforum

Conference Proceedings Paper

Nitrogen Rich Stainless Steel Coatings Obtained by RF Sputtering Process

Claudia Borri, Stefano Caporali, Francesca Borgioli and Emanuele Galvanetto *

Department of Industrial Engineering, University of Florence, via S. Marta 3, 50139 Florence, Italy; claudia.borri@unifi.it (C.B.); stefano.caporali@unifi.it (S.C.); francesca.borgioli@unifi.it (F.B.)
* Correspondence: emanuele.galvanetto@unifi.it; Tel.: +39-055-2758-759

Received: 15 February 2019; Accepted: 6 March 2019; Published: 7 March 2019

Abstract: Magnetron sputtering is a useful tool for producing coatings on various substrates at low temperature. The use of an austenitic stainless steel target in a nitrogen-containing plasma mixture allows to obtain nanostructured coatings with the formation of the so-called S phase, supersaturated interstitial solid solution of nitrogen in the expanded and distorted austenite lattice, which shows improved hardness and higher corrosion resistance in comparison with the bulk alloy. In the present research, RF magnetron sputtering deposition of austenitic stainless steel coatings using an AISI 316L target in nitrogen-containing plasma gas was studied. The effect of the N_2/Ar gas ratio and the deposition temperature on nitrogen content, phase composition and crystallite size is investigated by mean of XPS, XRD and electron microscopy analyses. The results show that the nitrogen content in the resulting deposit slightly depends on the N_2/Ar ratio in the chamber during the deposition, reaching a maximum value of about 35% with a 30% N_2/Ar gas composition mixture in the chamber. Data obtained on different substrates are presented and a preliminary evaluation of the corrosion resistance behaviour is also reported.

Keywords: expanded austenite; RF reactive sputtering; nanostructured coatings

1. Introduction

Austenitic stainless steels are widely used in many industrial fields because of their very high general corrosion resistance; nevertheless, they can suffer pitting or crevice corrosion in specific environments and their low hardness and wear resistance can limit the number of possible industrial applications. Among the more recent surface treatments low temperature plasma nitriding has received increasing attention as surface ◎modification due the forming of a supersaturated interstitial solid solution of nitrogen in the expanded and distorted γ-Fe f.c.c. lattice, (known as S phase or expanded austenite) improving surface hardness, wear resistance and corrosion resistance in chloride-ion solutions [1,2]. Moreover, this surface modification influences also water wettability [3] and biocompatibility [4,5].

Reactive magnetron sputtering is one of the techniques that can be used for S-phase layer production even at a very low temperature [6–9] with constant nitrogen content and also reducing the risk of S-phase decomposition or nitride formation. The main objective of this study is to investigate an influence of two principal process's parameters: temperature and nitrogen content on S-phase layer formation during reactive magnetron sputtering deposition on different substrates.

2. Materials and Methods

Substrate samples (30 mm × 15 mm × 1 mm) were obtained by a Si (100) wafer and from a stainless steel AISI 316L sheet plate (finish BA) which nominal composition is reported in Table 1.

Table 1. Nominal composition of AISI 316L SS.

Designation			Chemical Composition wt.% (Max unless Stated)								
UNS No.	SAE No.	AISI No.	C	Si	Mn	P	S	Cr	Mo	Ni	Others
S31603	30316L	316L	0.030	0.75	2.00	0.045	0.030	16.0/18.0	2.00/3.00	10.0/14.0	N 0.10

Before the deposition the substrates were cleaned with isopropyl alcohol. Stainless steel thin films were deposited by RF magnetron sputtering (Korvus Technology HEX system with RF source at 13.56 MHz, Korvus Technology, Newington, UK) not biased and with a rotating sample holder equipped with a temperature controlled heater. The AISI 316L target of 50 mm in diameter and 1 mm in thickness obtained by the same sample sheet plate.

Three set of samples were obtained varying different parameters: the films were obtained at two different deposition temperature i.e. room temperature (RT) and 300 °C using different RF sputtering source power density values (2.0, 2.5 and 3.5 W cm^{-2}) and different Ar/N_2 gas ratio. The deposition distance was set constant at 8 cm. After initial high vacuum pumping the working pressure was set at 5 × 10^{-3} mbar. The film thickness was evaluated through a quartz crystal microbalance and since the deposition rate is dependent on the N_2 concentration (0.6 Å/s for N_2 = 0; 0.5 Å/s for N_2 = 15 vol.%, and 0.4 Å/s for N_2 = 30 vol.%), the deposition time was varied accordingly to obtain the desired thickness of the layer of approximately 400 nm.

The film morphology was investigated by field emission GAIA 3 TESCAN FIB-SEM (TESCAN Brno, Brno, Czech Republic), while its composition was determined by XPS analysis. For XPS measurements the samples were cleaned in ultrasonic cleaner with acetone for 30 min and then inserted in the UHV XPS chamber. The XPS instrument uses a non-monochromatic X-ray source (VSW Scientific Instrument Limited model TA10, (V.S.W. SCIENTIFIC INSTRUMENTS LIMITED, Manchester, UK); Al Kα radiation, 1486.6 eV and Mg Kα 1253.6 eV radiation) operating at 12 kV and 12 mA. A hemispherical analyser (VSW Scientific Instrument Limited model HA100) equipped with a 16-channel detector and dedicated differential pumping system was used for spectra acquisition. The spectra ware analysed by using CasaXPS software (Ver. 2.3.19PR1.0) after inelastic background subtraction using Shirley's method [10] and a mixed Gaussian and Lorentzian contributions used for each component. The spectra were calibrated by using internal standard of the adventitious C 1*s* transition at 284.8 eV [11].

The XRD analysis was performed by using a Bruker D8 Advance (Bruker Corporation, Billerica MA, USA); Cu Kα radiation, in Bragg-Brentano and Grazing Angle geometry and Philips X'Pert HighScore Plus (Ver. 2.2.4) and Maud software packages (Ver. 2.78).

Preliminary corrosion behaviour was studied in 5% NaCl aerated solution at room temperature by means of the potentiodynamic method. Polarization tests were performed using a standard three-electrode flat cell, equipped with an Ag/AgCl reference electrode (3.5 M KCl) and a platinum grid as counterelectrode with a potential scan rate of 0.3 mV s^{-1} after 18 h delay time. The sample surface area exposed to the electrolyte was 1 cm^2.

3. Results and Discussion

All the samples showed a mirror-like surface with a good adhesion to the substrate and uniform surface morphology. Samples of the same deposition batch showed no surface differences between the two kinds of sample substrates and only slight differences in surface topography was evidenced by electron scanning microscopy analysis.

Figure 1 shows typical sections of deposit on silicon wafer: it is possible to see the columnar nature of the film and its nano microstructure with smaller grains at the interface. The thickness is uniform and no microscopic defects or detachments have been revealed.

Two main features have been considered in the present study: the amount of incorporated Nitrogen inside the deposit and its form in terms of solution or nitride.

The nitrogen content as a function of RF power density is reported in Table 2. The results show that the quantity of nitrogen in the thin films is only slightly dependent by the power density in the studied range and it is found that it increases as the source power increases. The data are referred to films obtained at room temperature and with nitrogen fraction in the gas of 30 vol.%.

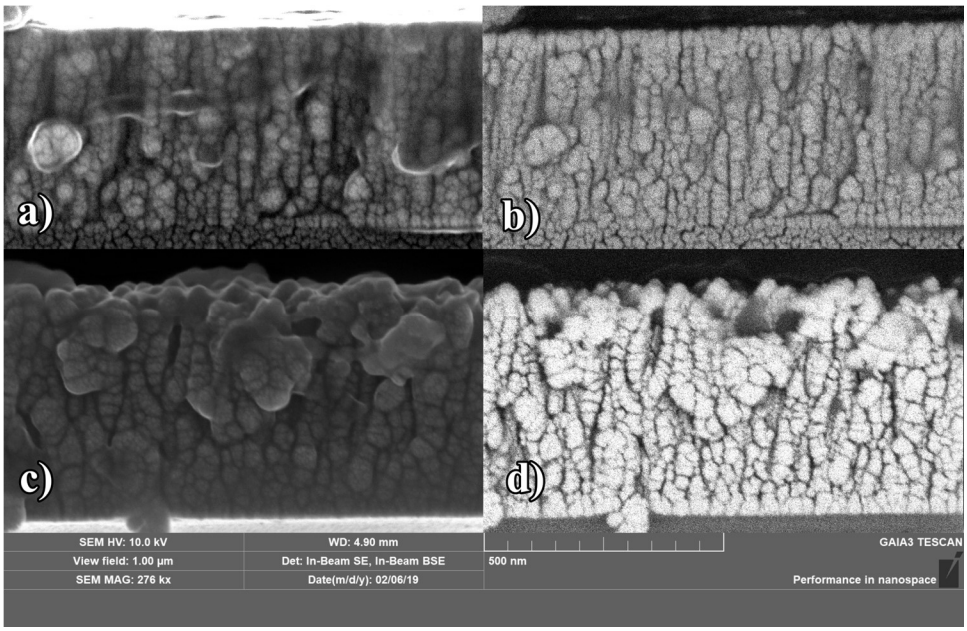

Figure 1. Cross section high resolution images of fractured films: (**a**,**b**) SE and BSE of 15% N_2, 300 °C, 3.5 W cm^{-2} sample; (**c**,**d**) SE and BSE of 30% N_2, 300 °C, 3.5 Wcm^{-2} sample.

Table 2. Nitrogen content as function of RF power. Samples obtained at RT and N_2 30 vol.% ratio. (In parenthesis the relative amount of Fe/Cr/Ni).

Power Density (W cm^{-2})	Composition (at %)			
	Fe 2*p*	Cr 2*p*	Ni 2*p*	N 1*s*
2.0	52.6 (74.0)	14.4 (19.8)	4.4 (6.2)	28.6 (–)
2.5	52.3 (73.3)	14.5 (20.0)	4.6 (6.7)	28.6 (–)
3.5	52.2 (73.3)	12.1 (17.7)	6.1 (9.0)	31.6 (–)

The nitrogen content as a function of the nitrogen gas content in the deposition chamber is listed in Table 3 (obtained at RT and 2.5 W cm^{-2} power density input).

As known from literature [12,13] the nitrogen content in the coating tends to increase as N_2/Ar ratio increases, while in our conditions this value is very slightly dependent on this parameter.

Table 3. Nitrogen content as function of plasma gas composition. Samples obtained at RT and 2.5 W cm^{-2} power input.

N_2/Ar Ratio (vol.%)	Composition (at %)			
	Fe 2*p*	Cr 2*p*	Ni 2*p*	N 1*s*
0%	79.4	16.7	8.9	0
15%	59.0	12.5	3.1	25.3
30%	52.3	14.5	4.6	28.6
50%	52.7	14.3	5.3	27.7

The effect of deposition temperature and nitrogen/argon volume ratio in the process was investigated at a fixed sputtering source power density of 3.5 W cm^{-2}. The results are summarized in Table 4.

The peak component at 396 eV, as reported in Figure 2, is due to the presence of nitrides, while the component at 402 eV is tentatively attributed to the presence of azides [14]. A more detailed analysis on the peak shape is under study.

Table 4. Nitrogen content as function of plasma gas composition RT and 300 °C.

N_2/Ar Ratio (vol.%)	N content (at %)	
	RT (25 °C)	300 °C
0%	–	–
15%	25.7	24.2
30%	31.6	34.4

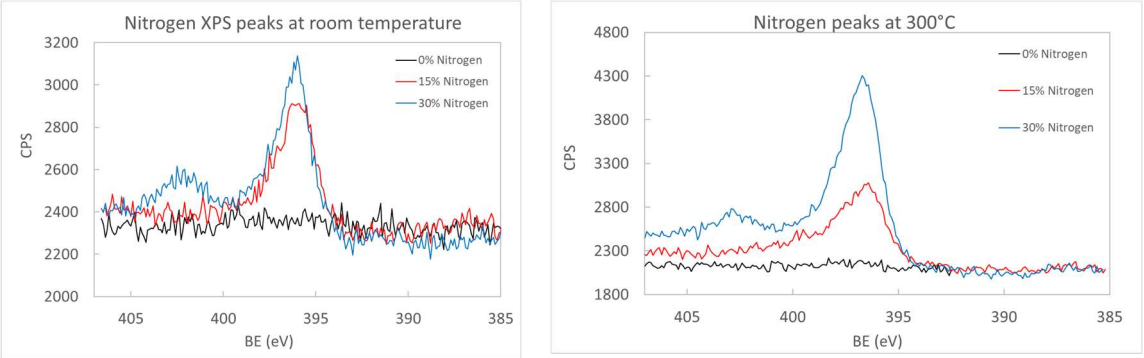

Figure 2. XPS spectra of N 1*s* peak for samples obtained with same parameters but at two different temperature varying the N_2/Ar ratio.

As known from literature [15,16], the relative amount of nickel in the film, as compared to the one in the original alloy, may vary due to preferential sputtering of the elements of the stainless steel target.

Figure 3 shows the grazing angle incidence X-ray diffraction patterns obtained from selected samples of these sets on silicon substrate. Although the AISI 316L stainless steel target has a face centered cubic (fcc) austenitic structure, metastable ferrite phase (a) with a body centered cubic (bcc) structure was formed in the pure stainless steel film deposited in pure argon gas and this is in agreement with literature data [9]. The ferrite films obtained at low temperature showed a preferred orientation of the (110) plane. As nitrogen, that is an austenite stabilizer, is incorporated in the film cubic fcc phase (austenite) is formed.

From the XRD data it is possible to describe the effect of the amount of nitrogen in the plasma gas that induce the increase in solute atoms. The incorporation of nitrogen not only stabilized but also led to lattice expansion of the austenite phase, as can be seen from the original lattice parameter. Such an fcc austenite phase with expanded lattice is consistent with the one that has also been found in low temperature-nitrided austenitic stainless steel surfaces and termed expanded austenite or S phase [17,18].

The shape of the peaks reveals that the nano size of crystallites and this is more affected by the Nitrogen content in the plasma than the deposition temperature. As visible in the scan, net shape peaks are obtained for samples deposited with 15 vol.% N_2. Increasing the nitrogen ratio, in our experimental condition, a finer structure, evolving in form of amorphous or nitride compound can be supposed and as elsewhere found [19]. The effect of deposition temperature for sample obtained with 15 vol.% N_2 evidences the different preferred orientations of the films. At room temperature deposit the preferred orientation is (111) while at 300 °C the samples showed a marked (200) preferred orientation.

As for the low temperature-nitrided austenitic stainless steel samples, also this cubic phase presents the well-known shift of (111) peak relative to the ideal cubic structure confirming the nature of the obtained films [19,20].

Amongst the various phases produced in SS–N films by reactive sputtering, the S phase is the most interesting since it provides a range of attractive mechanical and corrosion properties

Typical polarization curves of untreated and coated samples are shown in Figure 4.

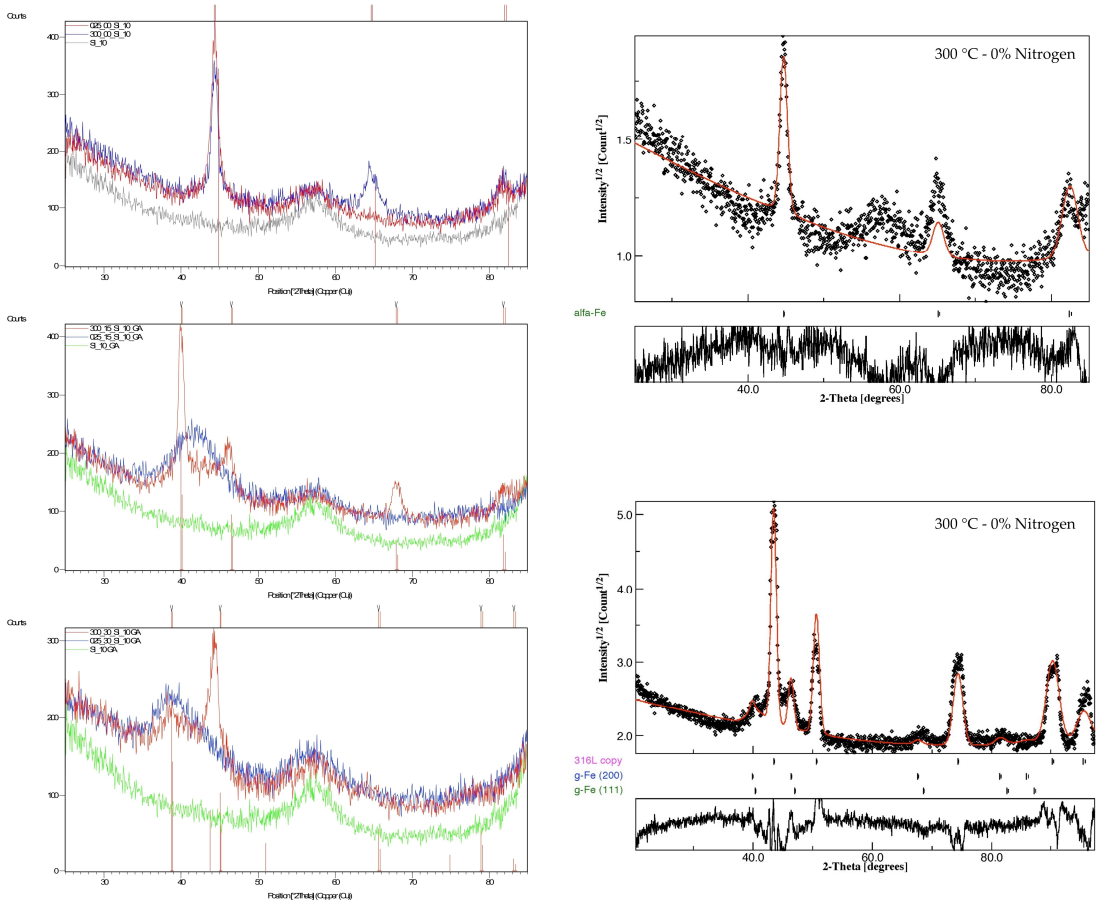

Figure 3. GA XRD scans of selected samples: (**a**) samples obtained at 0, 15 and 30 vol.% nitrogen on silicon substrate at different temperature; (**b**) selected samples on SS substrate at 300 °C and 0 and 15 vol.% N_2.

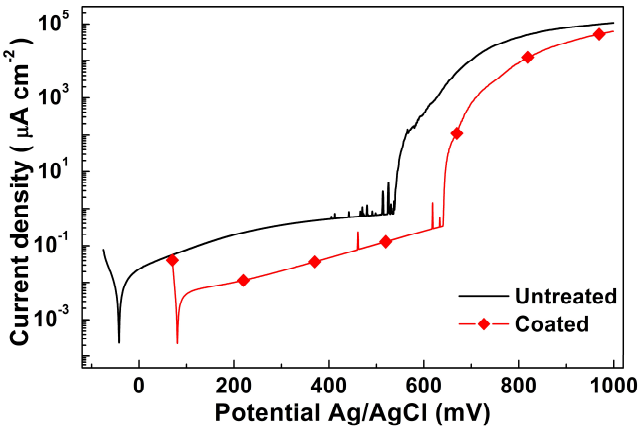

Figure 4. Polarization curves of untreated and coated samples (solution: 5% NaCl, aerated).

The untreated samples have a passive corrosion behaviour, with low anodic current density values, which rapidly increase owing to the occurrence of localized corrosion phenomena. After the tests the surface of the samples shows many deep pits, randomly distributed on the surface, and crevice corrosion is observable in the area shielded by the PTFE gasket.

The coated samples have a similar passive behaviour, but both corrosion and pitting potential values are higher and anodic current density in the passive branch is lower, in comparison with those of untreated samples, suggesting a better corrosion resistance

4. Conclusions

Amongst the various phases produced in SS–N films by reactive sputtering, the S phase is the most interesting since it provides a range of attractive mechanical and corrosion properties.

The use of an austenitic stainless steel as target in a nitrogen-containing plasma mixture allows to obtain nanostructured coatings with the formation of the so-called S phase, supersaturated interstitial solid solution of nitrogen in the expanded and distorted austenite lattice. In our experimental condition, nanostructured thin films consisting of S-phase are obtained. Increasing the nitrogen content in the plasma gas thin homogeneous films with a finer structure, evolving in form of amorphous or nitride compound have been produced.

Author Contributions: Conceptualization, E.G., F.B., S.C. and C.B.; Formal Analysis, E.G., F.B., S.C. and C.B.; Investigation, E.G., F.B., C.B. and S.C.; Writing–Original Draft Preparation, E.G.; Writing–Review & Editing, E.G. and S.C.; Project Administration, E.G.; Funding Acquisition, E.G. and S.C.

Funding: This research was funded by Regione Toscana within POR CreO Fesr 2014–2020, "Thin Fashon" project (CIP CIPE D55F17000240009).

Conflicts of Interest: The authors declare no conflict of interest.

References

1. Dong, H. S-phase surface engineering of Fe–Cr–Co–Cr and Ni–Cr alloys. *Int. Mater. Rev.* **2010**, *55*, 65–98.
2. Lo, K.H.; Shek, C.H.; Lai, J.K.L. Recent developments in stainless steels. *Mater. Sci. Eng. R Rep.* **2009**, *65*, 39–104.
3. Borgioli, F.; Galvanetto, E.; Bacci, T. Influence of surface morphology and roughness on water wetting properties of low temperature nitrided austenitic stainless steels. *Mater. Charact.* **2014**, *95*, 278–284.
4. Buhagiar, J.; Bell, T.; Simmons, R.; Dong, H. Evaluation of the biocompatibility of S-phase layers on medical grade austenitic stainless steels. *J. Mater. Sci. Mater. Med.* **2011**, *22*, 1269–1278.
5. Lin, Y.-H.; Lan, W.-C.; Ou, K.-L.; Liu, C.-M.; Peng, P.-W. Hemocompatibility evaluation of plasma-nitrided austenitic stainless steels at low temperature. *Surf. Coat. Technol.* **2012**, *206*, 4785–4790.
6. Dahm, K.; Dearnley, P. S phase coatings produced by unbalanced magnetron sputtering. *Surf. Eng.* **1996**, 12, 61–67.
7. Bourjot, A.; Foos, M.; Frantz, C. Basic properties of sputtered 310 stainless steel-nitrogen coatings. *Surf. Coat. Technol.* **1990**, *43–44*, 533–542.
8. Baranowska, J.; Fryska, S.; Suszko, T. The influence of temperature and nitrogen pressure on S-phase coatings deposition by reactive magnetron sputtering. *Vacuum* **2013**, 90, 160–164.
9. Kappaganthu, S. R.; Sun, Y. Influence of sputter deposition conditions on phase evolution in nitrogen-doped stainless steel films. *Surf. Coat. Technol.* **2005**, 198, 59–63.
10. Shirley, D.A. High-resolution X-ray photoemission spectrum of the valence bands of gold. *Phys. Rev. B* **1972**, *5*, 4709–4714.
11. Susi, T.; Pichler, T.; Ayala, P. X-ray photoelectron spectroscopy of graphitic carbon nanomaterials doped with heteroatoms. *Beilstein J. Nanotechnol.* **2015**, *6*, 177–192.
12. Terwagne, G.; Colaux, J.; Collins, G.A.; Bodart, F. Structural and quantitative analysis of nitrided stainless steel coatings deposited by dc-magnetron sputtering. *Thin Solid Films* **2000**, *377*, 441–446.
13. Shedden, A.B.; Kaul, N.F.; Samandi, M. The role of energetic neutrals in reactive magnetron sputtering of nitrogen-doped austenitic stainless steel coatings. *Surf. Coat. Technol.* **1997**, *97*, 102–108.

14. Sharma, J.; Gora, T.; Rimstidt, J.D.; Staley, R. X-ray photoelectron spectra of the alkali azides *Chem. Phys. Lett.* **1972**, *15*, 232–235.
15. Fryska, S.; Baranowska, J. Microstructure of reactive magnetron sputtered S-phase coatings with a diffusion sub-layer. *Vacuum* **2017**, *142*, 72–80.
16. Alresheedi, F.I.; Krzanowski, J.E. Structure and morphology of stainless steel coatings sputter-deposited in a nitrogen/argon atmosphere. *Surf. Coat. Technol*. **2016**, *314*, 105–112.
17. Fewell, M.P.; Mitchell, D.; Priest, J.M.; Short, K.T.; Collins, G.A. The nature of expanded austenite. *Surf. Coat. Technol*. **2000**, *131*, 300–306.
18. Li, X.Y. Low temperature plasma nitriding of 316 stainless steel—Nature of S phase and its thermal stability. *Surf. Eng.* **2001**, *17*, 147–152.
19. Kappaganthu, S.R.; Sun, Y. Formation of an MN-type cubic nitride phase in reactively sputtered stainless steel-nitrogen films. *J. Cryst. Growth* **2004**, *267*, 385–393.
20. Christiansen, T.; Somers, M. On the crystallographic structure of S-phase. *Scripta Materialia* **2004**, *50*, 35–37.
21. Sun, Y.; Li, X.; Bell, T. X-ray diffraction characterisation of low temperature plasma nitrided austenitic stainless steels. *J. Mater. Sci.* **1999**, *34*, 4793–4802.